CICE 2023 Rio de Janeiro – Brazil 11TH INTERNATIONAL CONFERENCE ON FRP COMPOSITES IN CIVIL ENGINEERING

EBR VS EBROG FOR FRP STRENGTHENING OF RC SLABS: EXPERIMENTAL AND NUMERICAL MODELLING

Enzo Martinelli, University of Salerno, IT, e.martinelli@unisa.it
Matteo Breveglieri, Empa, CH, matteo.breveglieri@empa.ch
Christoph Czaderski, Empa, christoph.czaderski@empa.ch
Niloufar Moshiri, Empa, nilou.msh@gmail.com

ABSTRACT

Fiber-Reinforced Polymer (FRP) strips are often utilized with the aim to enhance the bending capacity of Reinforced Concrete (RC) slabs, in view for the latter to either resist higher loads or face aging and damage issues. However, the weak link of Externally Bonded Reinforcement (EBR) is the adhesion between the FRP strip and the concrete substrate. Several studies, both experimental and theoretical were conducted to better understand the mechanical foundations and, thus, come up with effective technological solutions capable to avoid the so-called debonding failure between FRP and concrete. In this context, Externally Bonded Reinforcement on Grooves (EBROG) emerged as a convenient technology to enhance the bonding capacity of FRP strips glued on concrete. This paper summarizes the results obtained from three experimental tests carried out on 6-m-long RC slabs strengthened in bending by FRP strips glued according to either EBR or EBROG technique. Specifically, two slabs were strengthened by an EBROG FRP strip, which in one case was also prestressed before gluing. The experimental results demonstrate the higher capacity of EBROG with respect to the conventional EBR technique and some numerical analyses show that the observed mechanical behaviour can be easily interpreted by means of reasonably simple theoretical models.

KEYWORDS

FRP, Concrete, Debonding, Prestressing, Experimental tests, Numerical modelling, Externally Bonded Reinforcement (EBR), Externally Bonded Reinforcement on Grooves (EBROG), End Anchorage.

INTRODUCTION

It is generally agreed upon that improving reinforced concrete (RC) structures, which are frequently impacted by damage and aging phenomena, is more sustainable and cost-effective than demolishing and building new ones. Therefore, the development of innovative and efficient strengthening methods is a subject of current relevance in the field of structural engineering.

The strengthening technique described in this paper involves bonded carbon Fiber-Reinforced Polymer (FRP) strips as well a new all-FRP end-anchor system. The introduced innovations are based on the use of prestressed carbon FRP strips bonded on a grooved concrete surface according to the Externally Bonded on Grooves (EBROG) method [1], along with a newly developed all-FRP end-anchor system intended to further improve the bond resistance at the end of the strip.

The strengthening procedure was patented by S&P Clever Reinforcement and Empa [2-3]. Figure 1 briefly shows the differences between the Externally Bonded Technique (EBR) and the aforementioned EBROG technique. Specifically, the EBR technique, which is the standard solution for bonding FRP strips to concrete surfaces, the strip is simply bonded through an epoxy-based adhesive spread out on a previously ground and cleaned concrete surface. Although EBR has been widely employed in practice, it often results in limited bond resistance, which affects the actual effect of FRP on the capacity of strengthened RC members.

An improvement of the bond strength between concrete and FRP was achieved by introducing the EBROG method, which was initially developed at Isfahan University of Technology (IUT) and was later applied at Empa [4] in conjunction with prestressed CFRP. This more recent technique requires the creation of tiny grooves on the concrete surface (Figure 1b) which are later filled with epoxy

adhesive. The bond strength improves significantly as demonstrated by several investigations [4]. As a general rule, it is possible to affirm that the EBROG mobilizes a four-time larger concrete's specific fracture energy in comparison to the EBR [5]. However, this factor depends on the size, shape and number of grooves. Before grooving, it is recommended to prepare the same concrete surface preparation as in the case of EBR. As depicted in Figure 1b, in addition to the adhesive in the grooves a small layer of adhesive is placed between concrete soffit and FRP strip, like in the EBR technique. Conversely, in comparison to the near-surface mounted (NSM) technique, in which the FRP is placed inside the grooves, in the EBROG technique requires narrower grooves (~10 mm in depth), which makes it possible to adopt this technique in RC members with a reduced concrete cover.

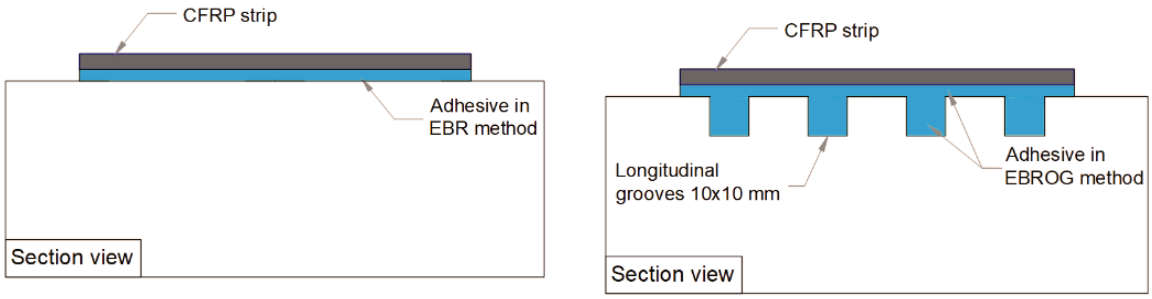

(a) EBR *(b) EBROG*

Figure 1: EBR (externally bonded reinforcement). EBROG (EBR on grooves).

EBROG AND END-ANCHORAGE

Despite the excellent bond between concrete and FRP exploited by the EBROG technique, end-anchorages are required for pre-stressed CFRP strips with the aim to transfer the prestressing forces to the main concrete substrate. Preliminary experiments in which 2-U-shaped carbon-FRP (CFRP) “staples” were used to anchor prestressed FRP strips were presented in [4]. The results demonstrated the feasibility of the new anchorage system in conjunction with the EBROG method for a modest value of prestressing force equal to 100 kN (corresponding to an axial strain of 4.6 ‰).

However, in the present work, the initial prototype of end anchorage was further developed to increase the prestressing force to 140 kN, to achieve comparable performance as the prestressed CFRP strips with metallic end-anchorage plates. The improvement of the prototype was possible through full-scale lap-shear tests, i.e. real anchorage size and forces. Figure 2 shows the final layout of the end anchorage. The metallic bolts are required to secure the prestressing setup (clamps, hydraulic cylinder), but they are eliminated after the CFRP strip is applied.

Figure 2: Final layout of the new end-anchorage before the test

EXPERIMENTS

The novel end-anchorage underwent a systematic evaluation through lap shear tests, where several layouts were tested by modifying the size and number of the grooves, as well as the size and number of the staples. Subsequently, the end-anchorage layout that proved to be the most effective was chosen,

and large-scale slab testing was conducted extensively to demonstrate its feasibility and assess its performance.

Full-scale lap-shear tests

The end-anchorage was developed through experiments involving the release of prestress forces, which are referred to as the "prestress force release" experiments. The experimental setup is illustrated in Figure 3. The CFRP strip is prestressed and glued with epoxy resin over a bond length of 300 mm to a concrete block. After the curing of the epoxy adhesive, the prestressing force is released on one side until debonding failure occurs. The difference between the initial force and the force just before failure on the releasing side indicates the end-anchorage resistance. By conducting these experiments, it was possible to determine the consequences of EBR and EBROG techniques as well as other parameters like the number and size of U-shaped CFRP staples on the end-anchorage resistance. In a previous study, the principle of performing prestress force release tests is explained in detail [6].

(a) (b)

Figure 3: (a)Test set-up for the small-scale experiments, (b) after failure

Large scale tests

To gain practical experience and compare structural performance, the newly developed end-anchorage method was utilized on a 1.00 m wide, and 0.22 m high RC slab spanning on support-to-support distance of 6.00 m (overall beam length being 6.50 m). In comparison to unstressed EBR and unstressed EBROG specimens, the test program in Table 1 was conducted and the adopted setup for a 6-point bending test setup is depicted in Figure 4. Further information regarding these experiments can be found in [7].

Table 1: Test program of the large-scale experiments.

Slab No.	CFRP strip	concrete surface	End-anchorage
1	100x1.4mm, unstressed	EBR	No
2	100x1.4mm, unstressed	EBROG	No
3	100x1.4mm, prestressed (140kN)	EBROG	U-shaped anchors

Figure 4: Test set-up for the large-scale experiments.

RESULTS AND DISCUSSION

Full-scale lap-shear tests

Figure 5 presents some of the results obtained from lap-shear experiments, indicating that EBR (T1-EBR) does not possess adequate resistance to withstand a prestressing force of 140 kN, as it fails well before the target force. The utilization of the EBR method together with 2- U-shaped staples did not lead to a noteworthy increase in the resisting force (T2-EBR(2U). However, it can be observed that capacity significantly increases in the case of EBROG specimens. Moreover, to ensure a higher increase in strength and a wider safety margin, additional U-shaped CFRP staples were added. Figure 5 shows that the force increase by increasing the number of U-shaped staples. The final design includes three U-shaped CFRP staples, resulting in an end-anchorage resistance of approximately 260-270 kN, providing a safety margin of 1.9 to the prestressing force of 140 kN (T7-EBROG (3U), T8-EBROG (3U) [8].

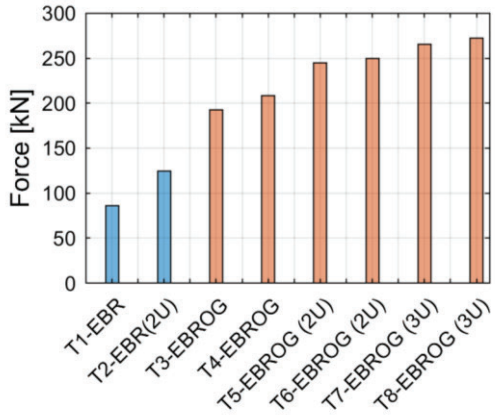

Figure 5: End-anchorage resistance (each column represents one test result).

Large scale tests

Figure 6 displays the load-displacement and load-CFRP strip strain behaviour of three large-scale failure tests. A total of four CFRP staples were utilized in the final arrangement of the EBROG slabs. The first slab, which was strengthened with unstressed EBR, had a load capacity of about 100 kN and a maximum strain in the CFRP strip of around 7.5 ‰. The second slab, strengthened with unstressed EBROG, had the same load capacity as the third slab, which was strengthened with prestressed EBROG (about 130 kN). Both slabs had a similar CFRP strip strain at maximum load of approximately 12.5 ‰.

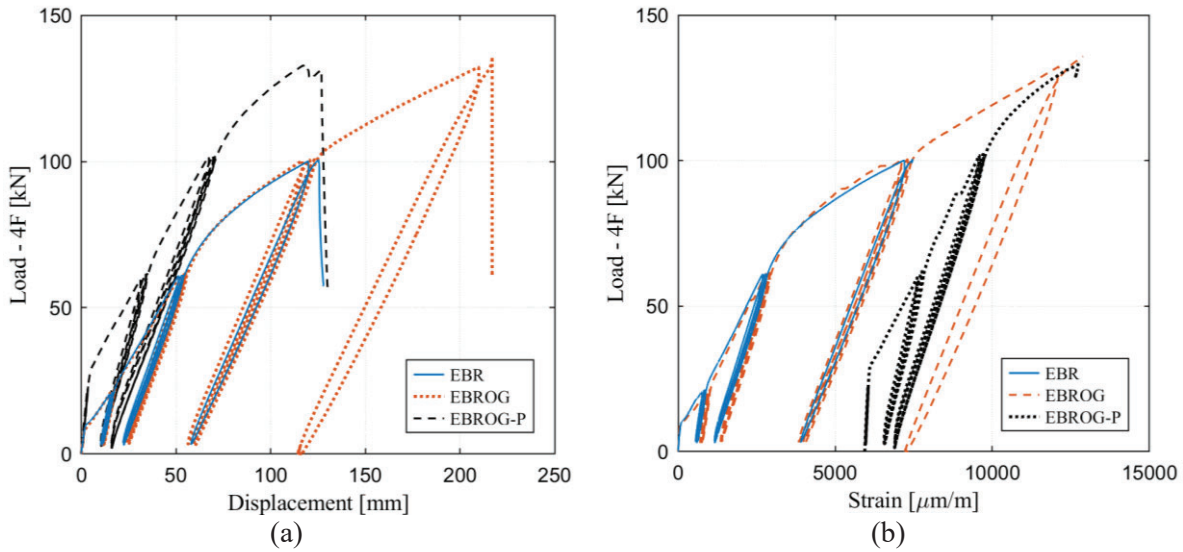

Figure 6: Load-displacement and Load-CFRP strip strain diagram of the large-scale experiments.

In all cases, the failure modes observed were related to the detachment of the CFRP strip from the concrete surface. However, it should be noted that the two slabs with EBROG exhibited an additional failure mode characterized by partial tensile fracture of the CFRP strips. The load strain trajectories of the maximum measured strain on the CFRP strip are depicted in Figure 6b. Interestingly, the two EBROG slabs showed a maximum strain value at failure of approximately 12.5‰, which is close to the fracture strain of the CFRP strips (16‰.). This finding supports the assumption that the CFRP strips experienced a partial tensile fracture. More information regarding the experimental results can be found in [7].

NUMERICAL STUDY

Summary about the numerical model

Numerical analyses can be proposed with the aim to enhance the level of understanding of the mechanical phenomena that control the observed behaviour of the tested RC slabs. Specifically, the numerical procedure employed for this aim is an extension of the model already proposed in a previous study [8], with the addition of external prestressing in the FRP strip [10]. Moreover, effects of the possible interface slips between the FRP strip and the concrete substrate are simulated as part of a partial-interaction two-layer composite beam theory [11]. Therefore, the main kinematic assumptions of the present model are listed below:

- the RC slab is modelled as a Timoshenko beam, while the FRP strip is only characterized in terms of axial stiffness;
- the RC slab and the FRP strip may exhibit relative axial displacements (slips), but relative transversal displacements are restrained.

Based on these assumptions, an "exact" 2-node beam-like Finite Element can be derived, which is capable of simulating the linear elastic response of two-layer composite beams in partial interaction like the one under consideration [11]: it is characterized by 3 degrees of freedom (namely corresponding to the transversal displacement v, the rotation φ and the relative interface slip s) for each element, at the two end nodes i and j. It is worth to highlighting that, in the adopted model, the interface stiffness is set to (numerical) zero in the first elements representing the strengthened part of the slab. Moreover, in the case of the EBROG_P system, the interface slips at node 2 (schematically corresponding to the position of the end stirrups represented in Figure 2) are set to zero, with the aim to realize the actual boundary condition realized by the presence of the three stirrups.

Nonlinear stress-strain relationships are assumed to describe the mechanical behaviour of materials and are introduced in the FE model by following a well-known fiber approach and a secant incremental-iterative procedure implemented in a Matlab code [12]. Specifically, as already assumed in a previous work, concrete in compression is simulated by assuming a Sargin stress-strain law (with a linear-brittle branch in tension), whereas steel of rebars is modelled by assuming an elastic-plastic-hardening law. As for the FRP strip, a simple linear elastic brittle behaviour is assumed, which is characterized by given values of Young Modulus E_f and an ultimate strain $\varepsilon_{f,u}$.

The bond-slip laws assumed to simulate the full range response of the FRP-to-concrete interface have different shapes for EBR and EBROG systems. In fact, although the assumption of bi-linear (triangular) bond-slip laws is generally accepted in the literature, recent studies have shown that EBROG systems are characterized by a tougher behaviour with respect to similar EBR systems. Therefore, the adoption of a trilinear (trapezoidal) bond-slip law appeared more accurate in simulating the behaviour observed both in lap-shear and prestress-release tests of FRP strips glued to concrete through an EBROG solution. Figure 7 shows the two types of curves and emphasizes the main mechanical quantities that define each of them.

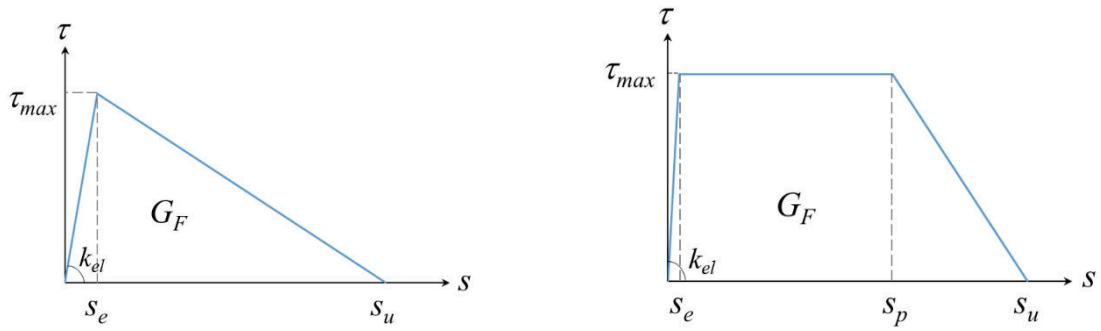

Figure 7: Bond-slip laws for the FRP-to-concrete interface: (a) EBR system, (b) EBROG system.

Details about the numerical algorithms are omitted for the sake of brevity; however, the present procedure follows the same nonlinear solution approach fully described in a previous paper [5-9].

Results and discussion

The tested slabs can be simulated by assuming a consistent set of values for the mechanical parameters that define the materials and the bond slip law. Table 2 summarizes all the values assumed for the main properties of materials assumed in the numerical analyses, namely structural concrete (i.e. mean compressive strength f_{cm}, mean tensile strength f_{ctm}, and Young modulus E_{cm}), rebar steel (i.e. Young modulus E_s, yielding and ultimate stresses, f_{sy} and $f_{s,u}$, respectively, plastic plateau and ultimate axial strains, $\varepsilon_{s,p}$ and $\varepsilon_{s,u}$, respectively), and FRP strip (i.e. Young modulus E_f, ultima axial strain $\varepsilon_{f,u}$ and possible initially imposed axial strain $\varepsilon_{f,pre}$ for prestressed FRP). It is worth highlighting that all the mechanical parameters summarised in Table 2 have been measured experimentally [13].

Table 2: Relevant mechanical parameters assumed for the materials.

Slab	Concrete			Steel					FRP		
	f_{cm} [MPa]	f_{ctm} [b] [MPa]	E_{cm} [b] [MPa]	E_s [MPa]	f_{sy} [MPa]	$\varepsilon_{s,p}$ [-]	$f_{s,u}$ [MPa]	$\varepsilon_{s,u}$ [-]	E_f [MPa]	$\varepsilon_{f,u}$ [-]	$\varepsilon_{f,pre}$ [-]
EBR	38.00	2.90	32837								-
EBROG	33.00	2.56	31476	210000	550	0.030	640	0.060	168000	0.014	-
EBROG_P	35.00[a]	2.70	32036								0.00595

[a] Determined from the cubic strength, using a conversion factor of 0.8
[b] Estimated from [13]

Moreover, Table 3 reports the parameters highlighted in Figure 7 for the two types of bond-slip laws assumed for EBR and EBROG FRP-to-concrete interface. It is worth highlighting that, for the sake of mechanical consistency, the same bond slip law is assumed for the two EBROG FRP slabs, as it is assumed that the attached materials have the same properties in the two specimens (regardless of the slight difference in f_{cm} assumed for the two slabs and reported in Table 2).

Table 3: Relevant mechanical parameters defining the bond-slip laws.

Slab	k_{el} [N/mm^3]	G_F [N/mm]	s_e [mm]	τ_{max} [MPa]	s_p [mm]	s_u [mm]
EBR	250	0.35	0.025	3.5	-	0.2
EBROG	200	3.19		5.00	0.50	0.80
EBROG_P						

Figure 8 shows the results of the analyses carried out by assuming the parameters reported in Tables 2 and 3. Specifically, it represents the force (4F) vs. displacement (at midspan) relationship for the three tested slab strips. The reference specimen (the slab with no FRP strengthening) was also simulated for the same of completeness, although it was not tested. The comparison between the experimental results and the corresponding numerical simulation shows that they is very good agreement in terms of both shape of the overall force-deflection curve, and also in terms of predicted failure mode (debonding for EBR and FRP rupture in tension for EBROG systems). It is worth highlighting that all the main stages of the structural response (e.g. cracking, yielding and failure) are taken with more than reasonable accuracy, which not only corroborates the predicting potential of the numerical model, but also (and more importantly) it points out that the tested slab exhibit a mechanically intelligible behaviour.

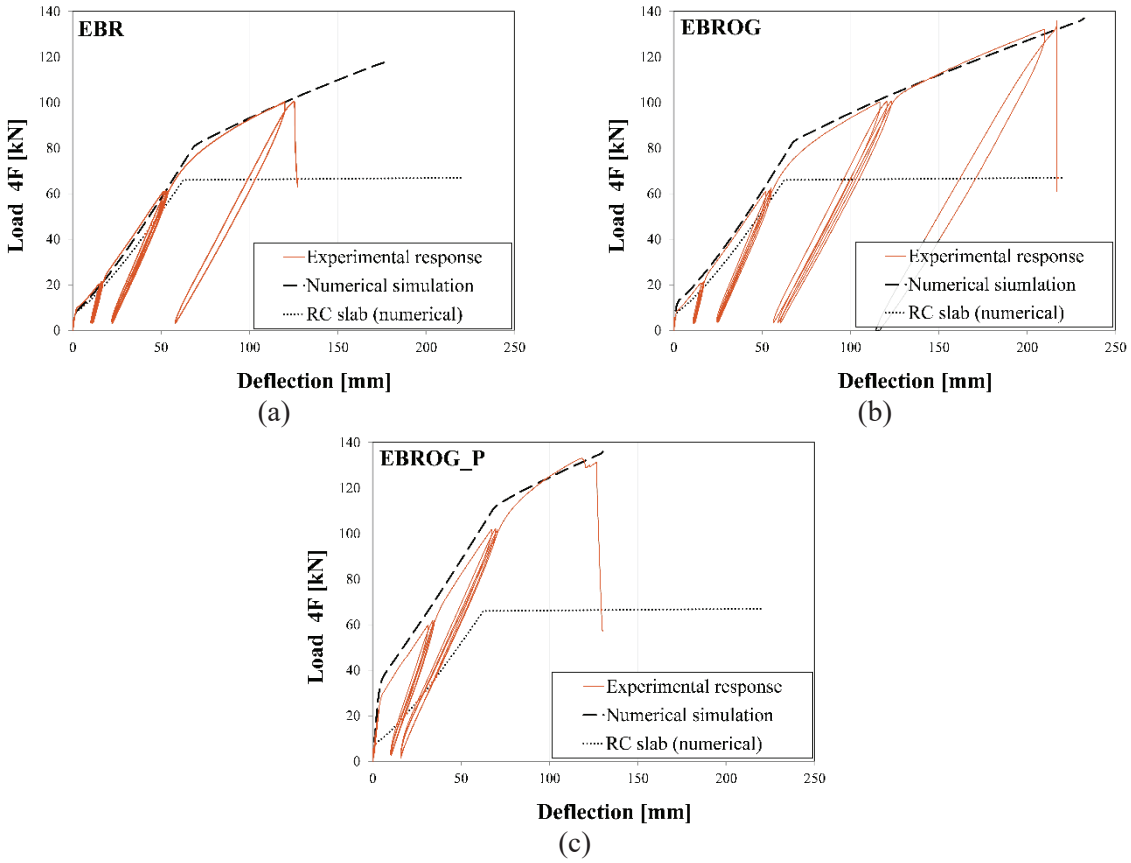

Figure 8: Force vs. deflection at midspan: (a) EBR, (b) EBROG, c) EBROG_P

A further comparison can be proposed in terms of relationship between the applied force (4F) and the resulting axial strain variation in the FRP strip at midspan (Figure 8). The agreement between experimental measurements and numerical results is almost complete and confirms that the model can reproduce the overall response of the structural systems under consideration.
Figures 8 and 9 demonstrate that the numerical model are in very good agreement with the obtained experimental results, as the values of both the maximum deflection and the maximum axial developed in the FRP strip are very close to the corresponding experimental values.
However, both Figures 8a) and 9a) show that the numerical prediction of the ultimate load (as well as the corresponding midspan displacement and FRP axial strain) is higher than the values observed in the experimental tests. In fact, the determination of the ultimate load in the cases of debonding failure of the FRP strip is highly influenced by the value assumed for the interface fracture energy G_F as highlighted by Figure 10.

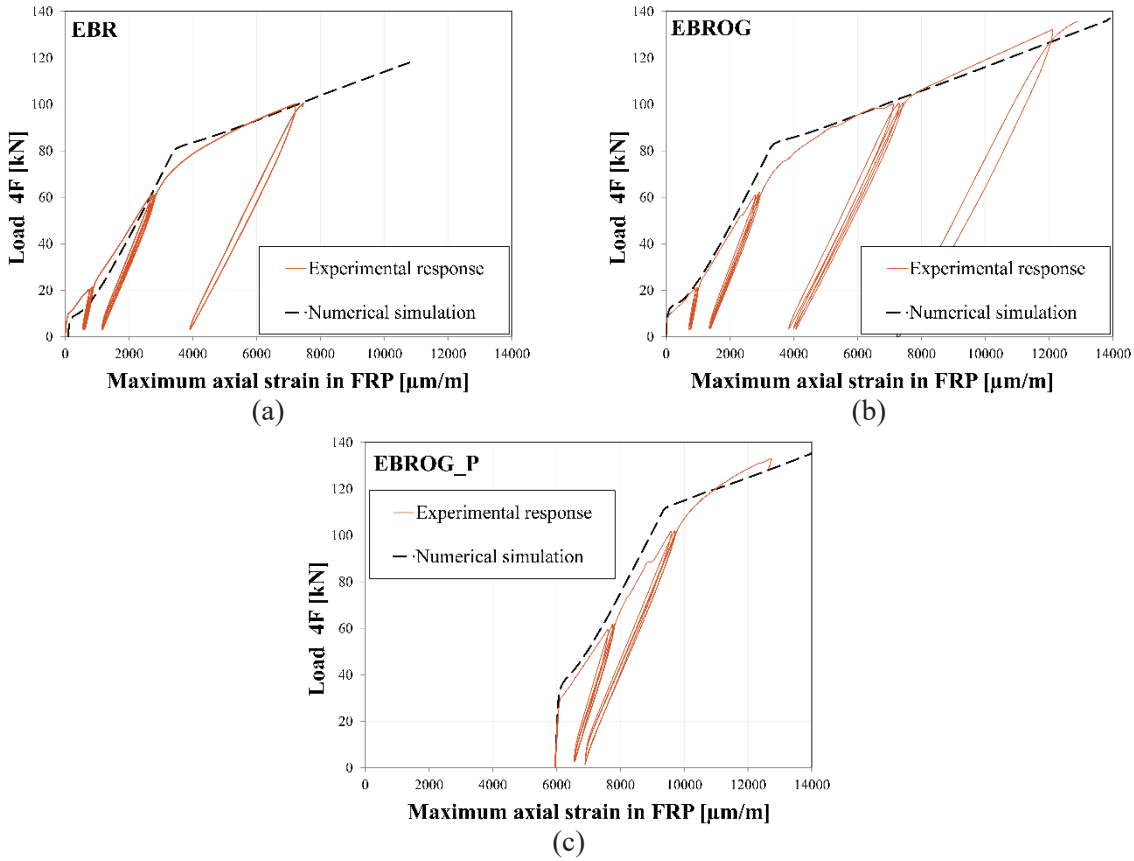

Figure 9: Force vs. FRP axial strain at midspan: (a) EBR, (b) EBROG, c) EBROG_P

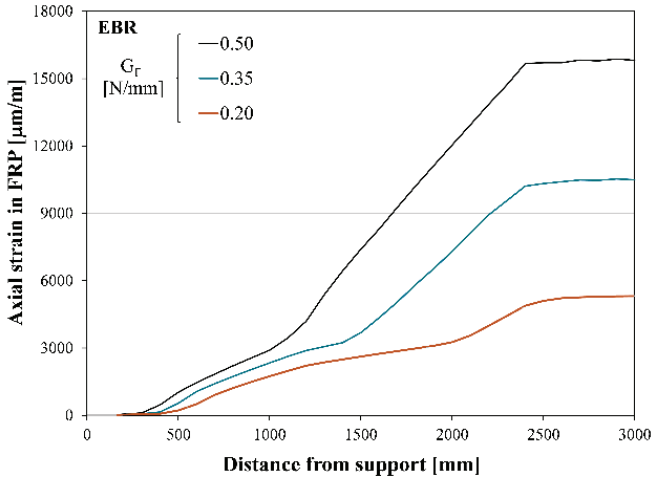

Figure 10: Axial strain distribution in the EBR FRP strip under ultimate load for variable G_F values.

The value G_F=0.35 N/mm assumed in the current simulation (which led to the results in Figures 8a and 9a) is reduced to 0.20 N/mm and raised to 0.50 N/mm. The obtained numerical results show that the maximum axial strain (5313 µm/m) obtained for G_F=0.20 N/mm is lower than the one observed experimentally (about 7300 µm/m, after Figure 9a), which means that the value of G_F that would have led to the best agreement between experimental results and numerical simulations in Figure 9a would be included in the range [0.20; 0.35] N/mm.
Conversely, an interface characterised by a G_F=0.5 N/mm would have led to maximum axial strains in the FRP strip (15810 µm/m, after Figure 10) that are actually higher than the ultimate axial strain

capacity of FRP: in other words, if G_F were equal to 0.5 N/mm, then failure would be due to FRP rupture instead of the debonding failure observed both experimentally and in the simulations for GF equal to either 0.20 N/mm and 0.35 N/mm.
Moreover, observing the distribution of axial strains throughout the longitudinal direction of the FRP-to-concrete interface reveals the intrinsic differences between the three bonding systems under consideration in this paper.
Figure 11 shows those distribution of axial strains simulated under the action of the maximum load (obtained from the numerical analyses). It shows that the higher capacity of the EBROG interface with respect to the EBR one results, as expected, in higher values of the FRP strain developed throughout the EBROG FRP strip and, consequently, higher values of the ultimate load than the EBR system (as already understandable by comparing Figure 8a and Figure 8b).
Moreover, the effect of the prestressing action on the axial strain distribution obtained at failure in the EBROG_P FRP strip is clearly visible by comparing the curves related to EBROG and EBROG_P in Figure 11. Specifically, the latter departs from a non-zero value, which is basically equal to the value $\varepsilon_{f,pre}$ reported in Table 2 and, after a transition along the longitudinal direction, reduces to the value achieved also in the EBROG FRP strip, as in both cases (EBROG and EBROG_P) failure occurs due to FRP rupture in tension. The non-zero value at the end of the FRP strip in the EBROG_P system is possible because of the action of the stirrups (Figure 2) that realise the end anchorage of the prestressed FRP strip.

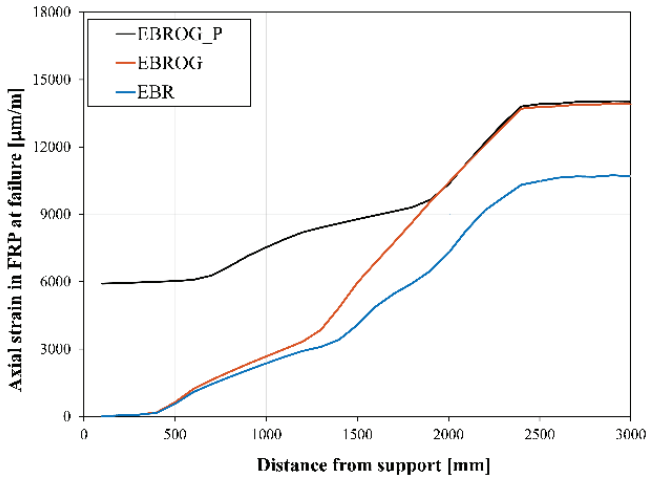

Figure 11: Axial strain distribution in the FRP strip under ultimate load.

CONCLUSIONS

The purpose of this paper is to introduce a novel approach for end-anchoring prestressed CFRP strips, which utilizes a combination of externally bonded reinforcement on grooves (EBROG) and newly developed U-shaped CFRP anchors. To develop this method, lap-shear prestressing force release tests were conducted, where various parameters, such as the geometry and number of U-shaped CFRP anchors, were examined to determine their impact on the end-anchorage resistance.
Furthermore, large-scale experiments were carried out to gain practical experience with the new end-anchorage method and compare its performance to unstressed EBR and unstressed EBROG specimens. These experiments revealed exceptional results, as the end-anchorage performed exceptionally well, even in cases of partial tensile fracture of the CFRP strips.
The proposed numerical simulations demonstrated that the observed experimental behaviour can be predicted on the bases of simple theoretical models, which makes easier the application of the tested technique for design purposes.
Further studies, both experimental and theoretical in nature, are planned with the aim to further understand the influence of the groove shape and patterns on the resulting behaviour of RC slabs with EBROG FRP strips.

ACKNOWLEDGEMENTS
The authors wish to acknowledge the Swiss Innovation Agency "Innosuisse" for their financial support for this research and development project (Project No. 37516.1 IP-ENG). Further thanks go to the Swiss National Science Foundation, which supported the stay of the first author at Empa (Scientific Exchange project IZSEZ0_202268/1). Lastly, the authors wish to acknowledge the industry partner S&P Clever Reinforcement Company AG for the support and collaboration in this project.

CITATIONS

[1] European patent EP 3 884 126, Method for strengthening concrete or timber structures using CFRP strips and concrete or timber structures strengthened by this method.

[2] Moshiri, N., Martinelli E., C. Czaderski C. (2022) Bond mechanism of nonprestressed and prestressed CFRP to concrete with EBR and EBROG methods, 5th International Conference Bond in Concrete 2022, Stuttgart, Germany.

[3] Mostofinejad, D. and Mahmoudabadi, E. (2010) Grooving as alternative method of surface preparation to postpone debonding of FRP laminates in concrete beams. Journal of Composites for Construction, 14(6): p. 804-811.

[4] N. Moshiri, C. Czaderski, D. Mostofinejad, A. Hosseini, K. Sanginabadi, M. Breveglieri, M. Motavalli (2020), Flexural strengthening of RC slabs with nonprestressed and prestressed CFRP strips using EBROG method. Composites Part B: Engineering, 201: 108359

[5] Moshiri, N., A. Tajmir Riahi, D. Mostofinejad, C. Czaderski and M. Motavalli (2019). Experimental and analytical study on CFRP strips-to-concrete bonded joints using EBROG method. Composites Part B: Engineering 158: 437-447.

[6] N. Moshiri, C. Czaderski, D. Mostofinejad, M. Motavalli (2021), Bond resistance of prestressed CFRP strips attached to concrete by using EBR and EBROG strengthening methods. Construction and Building Materials, 121209

[7] Moshiri N., E. Martinelli, M. Breveglieri and C. Czaderski, Experimental tests and numerical simulations on the mechanical response of RC slabs externally strengthened by passive and prestressed FRP strips, submitted in Feb. 2023 to Engineering Structures.

[8] Czaderski, C., N. Moshiri, E. Martinelli, M. Breveglieri, Strengthening of RC by prestressed CFRP strips Externally Bonded On Grooves, The 15th International Conference on Fibre-Reinforced Polymers for Reinforced Concrete Structures (FRPRCS-15) & The 8th Asia-Pacific Conference on FRP in Structures (APFIS-2022), 10th-14th December 2022, Shenzhen, China

[9] Faella C., Martinelli E., Nigro E. (2008), Formulation and validation of a theoretical model for intermediate debonding in FRP-strengthened RC beams, Composites Part B: Engineering, 39(4):645-655, https://doi: 10.1016/j.compositesb.2007.06.002;

[10] Michels J., Martinelli E., Czaderski C., Motavalli M. (2014), Prestressed CFRP strips with gradient anchorage for structural concrete retrofitting: Experiments and numerical modeling, Polymers, 6(1):114-131, https://doi: 10.3390/polym6010114;

[11] Martinelli E., Faella C., Di Palma G. (2012), Shear-Flexible Steel-Concrete Composite Beams in Partial Interaction: Closed-Form “Exact” Expression of the Stiffness Matrix, ASCE Journal of Engineering Mechanics, 138(2):151-163, https://doi: 10.1061/(ASCE)EM.1943-7889.0000320;

[12] MATLAB. version 9.9.0 (R2020b). Natick, Massachusetts: The MathWorks Inc.; 2020.

[13] European Committee for Standardization. Eurocode 2: Design of concrete structures - Part 1-1: General rules and rules for buildings Eurocode 2004.

CONFLICT OF INTEREST
The authors declare that they have no conflicts of interest associated with the work presented in this paper.

DATA AVAILABILITY
Data on which this paper is based is available from the authors upon reasonable request.